Nuclear-acoustic-resonance determination of the gradient-elastic tensor and indirect nuclear-spin interactions in niobium

J. Pellisson and J. Buttet*

Section de Physique, Université de Genève, Genève, Switzerland

(Received 22 July 1974)

Nuclear-acoustic-resonance studies of the absolute intensity of the signals and of the angular dependence of their second moments have been made in single crystals of niobium for the electric quadrupole transitions $\Delta m = \pm 1$ and $\Delta m = \pm 2$ as well as for the $\Delta m = \pm 1$ magnetic dipole transition. From the intensity measurements we find the two independent coefficients of the electric field gradient-elastic strain tensor to be $|S_{11} - S_{12}| = 1.2 \times 10^{16}$ and $|S_{44}| = 2.25 \times 10^{16}$ statcoulomb cm^{-3}. From the second-moment data we verify that the indirect effective spin Hamiltonian is the sum of an exchange and dipolar term. The pseudodipolar coefficients for the first and second nearest neighbors are equal to $B_1 = 180$ or -800 Hz and $B_2 = 0$ or -400 Hz. The pseudoexchange coefficients A_{ij} are such that $\Sigma_j A_{ij}^2 = 1.14$ kHz^2 corresponding to a first-nearest-neighbor coefficient $A_1 \simeq 300$ Hz. The contribution to the second moment of the indirect electric quadrupole spin Hamiltonian is also evaluated.

I. INTRODUCTION

The information given by the nuclear-acoustic-resonance (NAR) technique is in many ways similar to that given by nuclear-magnetic-resonance (NMR) studies in single crystals. However the NAR technique gives specific information, difficult to obtain by other methods, when the coupling between the sound wave and the nuclear spins is of electric quadrupole origin.

In the presence of strains the cubic symmetry at the nuclear position of an unstrained cubic crystal is destroyed and electric field gradients (efg) are created. The relation between the efg and the strains is represented by a fourth-rank tensor $\overleftrightarrow{S}$[1] (denoted efg-strain tensor) connecting the elastic strain tensor $\overleftrightarrow{\epsilon}$ and the efg tensor

$$V_{\alpha\beta} = \frac{\partial^2 V}{\partial \alpha \, \partial \beta} = S_{\alpha\beta,\gamma\delta} \, \epsilon_{\gamma\delta} \quad (\alpha,\beta,\gamma,\delta = x,y,z) \,,$$

$$(1)$$

where V is the potential at the site of the nucleus created by all electrons and neighboring ions. In metals the S-tensor components are difficult to measure. One method[2] used in aluminium[3] determines the S tensor by observing the broadening of an NMR line shape due to the presence of static applied strains and the stress fields around a dislocation. In another method, used for example in LiF,[4] acoustic waves at twice the Larmor frequency are generated in the crystal. The resulting periodic modulation of the interaction between the electric quadrupole moment of the nucleus and the efg induces transitions among the Zeeman energy levels. The transition rates are then measured by observing the rate of change of the amplitude of a standard (nonacoustic) NMR signal

and related to the S-tensor components. However, this method can not be used in metals, since only the nuclei in the skin depth of the electromagnetic wave contribute to the NMR signal and the elastic strains are not well known at the edge of the crystal. In the present method[5] the resonant absorption of acoustic energy by the nuclear-spin system is directly detected as a change $\Delta\alpha$ in the acoustic attenuation coefficient of the sound wave. When the coupling between the sound wave and the nuclear spins is the electric quadrupole coupling, an absolute measure of $\Delta\alpha$ allows us to determine the S-tensor components. This method has been used in alkali halides[6] and more recently in III-V semiconductors[7] and aluminium metal.[8] We give in Sec. II A the relation between the resonant change in acoustic attenuation $\Delta\alpha$ and the efg-strain tensor.

It is well known by NMR studies in metals that the dipole-dipole interaction between nuclear spins can not alone explain the line shapes and linewidths observed in heavy metals. It was first pointed out by Ruderman and Kittel[9] and Bloembergen and Rowland[10] that indirect interaction between the nuclear spins via the conduction electrons could contribute significantly to the linewidths. They showed that if the Fermi surface is assumed to have spherical symmetry, the indirect effective spin Hamiltonian H_{ij}^B between two nuclear spins $\vec{I}_i$ and $\vec{I}_j$ is the sum of an isotropic pseudoexchange interaction (or Ruderman-Kittel interaction) and a pseudodipolar interaction, which has the same form as the direct dipole-dipole interaction:

$$H_{ij}^B = A_{ij} \vec{I}_i \vec{I}_j + B_{ij}^{PP} [\vec{I}_i \vec{I}_j - 3(\vec{I}_i \vec{R}_{ij})(\vec{I}_j \vec{R}_{ij})R_{ij}^{-2}] \,,$$

$$(2)$$

where $\vec{R}_{ij}$ is the vector joining the nucleus i to

the nucleus j and A_{ij} and $B_{ij}^{p\,D}$ depend only on R_{ij}.

The pseudodipolar coefficients can be measured by continuous wave NMR. Van Vleck[11] has shown that the second moment of the NMR absorption line is not affected by the pseudoexchange term; it is thus possible to separate out the pseudodipolar contribution in a second-moment measurement. The pseudoexchange coefficients are however more difficult to obtain by NMR measurements. Alloul and Froidevaux[12] have related the modulation of the spin-echo envelope to the pseudoexchange coefficient. But this method gives unambiguous results only in the case of spin $\frac{1}{2}$, where the line shape is not broadened by static electric quadrupole interactions.

When the coupling between the sound wave and the nuclear spins is the dynamic electric quadrupole coupling, the NAR line shapes (and linewidths) differ from the NMR line shape. In the case of the Hamiltonian (2) and like spins, Loudon[13] has calculated the spin-phonon second moments for the transitions $\Delta m = 1$ (denoted by NAR1) and $\Delta m = 2$ (denoted by NAR2) which are both allowed by the electric-quadrupole-coupling mechanism. He finds that the second moment depends on the dipolar *and* exchange terms. For each direction of the magnetic field with respect to the crystal axes, it is then possible to extract separately the exchange and dipolar terms by measuring the second moments for the NMR, NAR1, and NAR2 perturbation Hamiltonians. We can then verify if the values of A_{ij} and $B_{ij}^{p\,D}$ for different orientations of the magnetic field are consistent with the predictions of the spin Hamiltonian (2), which has been assumed to be correct in all previous measurements.

In addition to the bilinear interaction H_{ij}^B, Kessel[14] has shown that there also exists an indirect interaction via the conduction electrons which has the form of an effective electric quadrupole interaction between the spins $\vec{I}_i$ and $\vec{I}_j$. Koloskova[15] has calculated the second moments in this case for NMR, NAR1, and NAR2 line shapes. This Hamiltonian, together with an effective quadrupole Hamiltonian via the phonon field,[16] could in principle also contribute to the second moments. We summarize the derivation of the effective spin Hamiltonian in Sec. II B and give the values of the second moments.

In this paper we report the experimental measurements of the S-tensor components and indirect interaction coefficients in the case of niobium single crystal. Previous measurements have shown that in niobium the transitions induced by the electric quadrupole[17] and magnetic dipole[18] interaction mechanisms between the sound wave and the nuclear-spin system are observable. This allows us to measure, by the NAR technique, not only the second moments of the NAR1 and NAR2 signals, but also that of the NMR signal which has the same line shape as the one due to the magnetic dipole mechanism. Schone[19] has already measured the second moments of the NMR line shapes in single crystals of niobium with magnetic field orientated along [001] and [110]. Our values are in good agreement with Schone's results where they can be compared. In Sec. III the experimental values of the S-tensor components, linewidths, and second moments are presented. We analyze the experimental data in Sec. IV and show in particular that the broadening of the lines is consistent with the Hamiltonian (2). The essential points of the paper are summarized in Sec. V.

II. THEORY

A. Electric quadrupole coupling

The nuclear electric quadrupole Hamiltonian is of the form

$$\mathcal{H}^Q = F \sum_{q=-2}^{+2} (-1)^q Q^q V^{-q}, \tag{3}$$

where $F = eQ/2I(2I-1)$, Q is the nuclear electric quadrupole moment, I is the nuclear spin, Q^q and V^q are defined as

$$Q^0 = 3(I^z)^2 - I(I+1),$$
$$Q^{\pm 1} = \mp \sqrt{\tfrac{3}{2}} (I^z I^{\pm} + I^{\pm} I^z), \tag{4}$$
$$Q^{\pm 2} = \sqrt{\tfrac{3}{2}} (I^{\pm})^2 ;$$

$$V^0 = \tfrac{1}{2} V_{zz}, \quad V^{\pm 1} = \pm (1/\sqrt{6})(V_{xz} \pm i V_{yz}),$$
$$V^{\pm 2} = (1/2\sqrt{6})(V_{xx} - V_{yy} \pm 2i V_{xy}). \tag{5}$$

The efg tensor $V_{\alpha\beta}$ will be used in three different contexts in this paper. When the electric quadrupole Hamiltonian describes the mechanism which induces transitions between the nuclear spins under the effect of the sound wave, $V_{\alpha\beta}$ is related to the strain tensor $\tilde{\epsilon}$ by the efg-strain tensor $\tilde{S}$ given in formula (1). A conduction electron, whose wave function is not of spherical (or cubic) symmetry around a nucleus, creates an efg at the site of the nucleus. The resulting electric quadrupole interaction, denoted by $h^{\text{quadr}}(l)$, is responsible for the conduction-electron quadrupole relaxation time and the electric quadrupole indirect interaction (see Sec. II B). Static efg, created by impurities or distortions in the crystal, may also exist at the site of a nucleus. They are responsible for the broadening of the linewidths mentioned in Sec. III A.

In NAR the relevant experimental quantity is the acoustic attenuation coefficient $\Delta\alpha$ for absorption of energy by a nuclear-spin system. In the case of an electric quadrupole coupling $\Delta\alpha$ is equal to $P_n/2P_0$, where P_0 is the incident acoustic power

per unit area and P_n is the power per unit volume absorbed by the nuclear-spin system:

$$P_n = \frac{N}{2I+1} \frac{h\nu}{kT} h\nu \sum_{m=-I}^{I-1(2)} W_{mm'},$$

where $m' = m + 1$ for a $\Delta m = \pm 1$ transition (NAR1) and $m' = m + 2$ for a $\Delta m = \pm 2$ transition (NAR2). N is the number of spins per unit volume, ν is the frequency of the sound wave, and $W_{mm'}$ the transition probability per unit time from the spin state m to the spin state m'. $W_{mm'}$ is proportional to the square of the matrix element $\langle m | \mathcal{H}^Q | m' \rangle$, which is easily calculated if we know $V_{\alpha\beta}$.[20]

In most of the experiments described in this paper transverse acoustic waves are propagated along the [110] direction of the crystal. For a given polarization direction, $V_{\alpha\beta}$ can be calculated using the transformation procedure described by Taylor[1] (also see Sundfors[7]) as a function of the orientation of the magnetic field. We have found that it is less confusing to work in the full tensor notation, using 9 by 9 matrices rather than 6 by 6 matrices as in the Vogt notation. In cubic symmetry three different S-tensor components describe the efg-strain tensor. In the Vogt notation they are S_{11}, S_{12}, and S_{44}. The number of independent components is reduced to two, if one assumes that the derivative with respect to the strain of the electronic charge at the nucleus is equal to zero.[21] Using Sundfors's notations[7] we write the acoustic attenuation coefficient $\Delta\alpha_1$ and $\Delta\alpha_2$, respectively, for NAR1 and NAR2:

$$\Delta\alpha_1 = CB_1 Q^2 f_1^2(\theta),$$

$$\Delta\alpha_2 = CB_2 Q^2 f_2^2(\theta), \tag{6}$$

where C, B_1, and B_2 have been defined in Ref. 7 and $f^2(\theta)$ is given in Table I for the different polarization directions and orientations of the magnetic field chosen. Some of the results in Table I had already been obtained in Refs. 7, 8, and 22

(there is a printing error in Table I of Ref. 8). On the same table we have given the angular dependence of $\Delta\alpha$ when the coupling between the sound wave and the nuclear spins is the magnetic dipole coupling.[23] In the case of niobium the electric quadrupole and the magnetic dipole coupling have the same order of magnitude; for an arbitrary direction of the magnetic field the $\Delta m = 1$ line shape is then the superposition of two resonance signals. This can be avoided if the magnetic field rotates in a plane perpendicular to the sound-wave vector ($\vec{H}_0$ in plane $\vec{\xi}$ and $\vec{q} \times \vec{\xi}$).

B. Indirect spin Hamiltonian and second moments

In what follows we will briefly summarize the derivation of the effective spin Hamiltonian between two spins $\vec{I}_i$ and $\vec{I}_j$. Consider a pair of nuclei at positions $\vec{R}_i$ and $\vec{R}_j$ and interacting individually with the conduction electrons. The electron-nuclear part of the Hamiltonian is given by

$$\mathcal{H} = \mathcal{H}_i + \mathcal{H}_j = \sum_l h_i(l) + h_j(l),$$

where the sum has to be taken on all conduction electrons and

$$h(l) = h^{\text{cont}}(l) + h^{\text{dip}}(l) + h^{\text{quadr}}(l).$$

$h^{\text{cont}}(l)$ is the usual Fermi-contact interaction, $h^{\text{dip}}(l)$ describes the dipolar interaction between the nuclear spin $\vec{I}_i$ and the electron spin, and $h^{\text{quadr}}(l)$ is given by Eq. (3) in which $V_{\alpha\beta}$ is now the efg tensor created by a conduction electron at position $\vec{r}_l$. The quadrupole relaxation time, first calculated by Mitchell,[24] arises from $h^{\text{quadr}}(l)$. By standard second-order perturbation theory and in the one-electron approximation, the effective spin Hamiltonian can be written

TABLE I. Coefficients $f_1^2(\theta)$ and $f_2^2(\theta)$ as defined by Eq. (6) and angular variation $f^2(\theta)$ of $\Delta\alpha$ in the case of a magnetic-dipole-type coupling. The sound-wave vector $\vec{q}$ is parallel to [110], the polarization vector $\vec{\xi}$ corresponds to a shear wave oriented along [001] or [1$\bar{1}$0]. θ is the angle between $\vec{q}$ and $\vec{H}_0$, ψ is the angle between [001] and $\vec{H}_0$.

$\vec{q} // [110]$		$f_1^2(\theta)$ NAR1	$f_2^2(\theta)$ NAR2	$f^2(\theta)$ NAR$_{\text{dip}}$
$\vec{H}_0$ in plane $\vec{q}$ and $\vec{\xi}$	$\vec{\xi} \| [001]$	$4(S_{44})^2 \cos^2 2\theta$	$(S_{44})^2 \sin^2 2\theta$	$\cos^4\theta$
	$\vec{\xi} \| [1\bar{1}0]$	$(S_{11}-S_{12})^2 \cos^2 2\theta$	$\frac{1}{4}(S_{11}-S_{12})^2 \sin^2 2\theta$	$\cos^4\theta$
$\vec{H}_0$ in plane $\vec{q}$ and $\vec{q} \times \vec{\xi}$	$\vec{\xi} \| [001]$	$4(S_{44})^2 \cos^2\theta$	$4(S_{44})^2 \sin^2\theta$	$\cos^2\theta$
	$\vec{\xi} \| [1\bar{1}0]$	$(S_{11}-S_{12})^2 \cos^2\theta$	$(S_{11}-S_{12})^2 \sin^2\theta$	$\cos^2\theta$
$\vec{H}_0$ in plane $\vec{\xi}$ and $\vec{q} \times \vec{\xi}$	$\vec{\xi} \| [001]$	$4(S_{44})^2 \cos^2\psi$	$4(S_{44})^2 \sin^2\psi$	$\cdots$
	$\vec{\xi} \| [1\bar{1}0]$	$(S_{11}-S_{12})^2 \sin^2\psi$	$(S_{11}-S_{12})^2 \cos^2\psi$	$\cdots$

$\Delta^2 E$

$$= \sum_{n \vec{k} s} \sum_{n' \vec{k}' s'} \frac{\langle n \vec{k} s \mid h_i \mid n' \vec{k}' s' \rangle \langle n' \vec{k}' s' \mid h_j \mid n \vec{k} s \rangle}{\epsilon_n(\vec{k} s) - \epsilon_{n'}(\vec{k}' s')},$$

(7)

where $\mid n \vec{k} s \rangle$ are Bloch states in the reduced-zone scheme, n representing the band, $\vec{k}$ the reduced wave vector, and s the spin state. The sum on $n \vec{k} s$ runs over all the occupied states and $n' \vec{k}' s'$ runs over the unoccupied ones. Following Bloembergen and Rowland's procedure, Mahanti and Das[25] have shown that, if we exclude the quadrupolar term, we obtain for the case of a spherical Fermi surface the Hamiltonian (2). If we then add the direct dipole-dipole interaction to Hamiltonian (2) we have

$$H_{ij} = A_{ij} \vec{I}_i \vec{I}_j + B_{ij} [\vec{I}_i \vec{I}_j - 3(\vec{I}_i \cdot \vec{R}_{ij})(\vec{I}_j \cdot \vec{R}_{ij}) R_{ij}^{-2}], \quad (8)$$

where the second term is now the sum of the dipole-dipole interaction and the pseudodipolar interaction, which is an oscillatory function of R_{ij} like the Ruderman-Kittel interaction. The main contribution to the pseudoexchange coefficient A_{ij} comes from $\langle \mid h_i^{\mathrm{cont}} \mid \rangle \langle \mid h_j^{\mathrm{cont}} \mid \rangle$ and the pseudodipolar contribution B_{ij}^{PD} to B_{ij} from $\langle \mid h_i^{\mathrm{cont}} \mid \rangle \langle \mid h_j^{\mathrm{dip}} \mid \rangle$. Under these assumptions each lattice shell p is characterized by two constants $A_p = A_{ij}(R_{ij})$ and $B_p = B_{ij}(R_{ij})$. Using the irreducible-tensor method, Hirst[26] has shown that if we relax the aforementioned assumptions, more than two constants may characterize an arbitrary lattice shell. In the bcc structure his calculation shows that two constants describe the first two shells and three constants the third shell. Thus the general Hamiltonian for the first two shells reduces to the Hamiltonian (8). The main contribution to A_{ij} and B_{ij} (see Sec. IV) comes from the two nearest shells, negligibly small deviations from Hamiltonian (8) are thus to be expected in niobium. In the fcc structure three constants already characterize the first shell, which has the same symmetry properties as the third shell in a bcc structure. In this case, from Hirst's work, stronger deviations from Hamiltonian (8) may be expected.

Kessel[14] has calculated the effective interaction Hamiltonian due to the term $\langle \mid h_i^{\mathrm{quadr}} \mid \rangle \langle \mid h_j^{\mathrm{quadr}} \mid \rangle$ in Eq. (7). Using the same approximations as Rudermann and Kittel he obtains the part of the Hamiltonian diagonal in energy:

$$H_{ij}^Q = C_{ij} \sum_{q=-2}^{+2} (-1)^q \bar{Q}_i^q \bar{Q}_j^{-q} + \sum_{q=-2}^{+2} \bar{D}_{ij}^{\mid q \mid} \bar{Q}_i^q \bar{Q}_j^{-q},$$

(9)

where $\bar{Q}^q$ is defined by Eq. (4) for a system of axis in which $\vec{H}_0$ is parallel to the z axis. C_{ij} is a function of R_{ij} only, whereas $\bar{D}_{ij}$ is a function of

R_{ij} and the angle $\bar{\theta}_{ij}$ between $\vec{R}_{ij}$ and $\vec{H}_0$. There are also crossed terms $\langle \mid h_i^{\mathrm{cont}} \mid \rangle \langle \mid h_j^{\mathrm{quadr}} \mid \rangle$ and $\langle \mid h_i^{\mathrm{dip}} \mid \rangle \langle \mid h_j^{\mathrm{quadr}} \mid \rangle$ in the spin Hamiltonian. Kessel has shown that they are negligible. The electric quadrupole relaxation rate is very small in most metals, and to our knowledge it has only been observed in molybdenum.[27] It is thus expected that the indirect electric quadrupole interaction will also be small. We will estimate in Sec. IV its contribution to the second moment in niobium and in molybdenum.

Following the work of Van Vleck,[11] Loudon[13] has calculated the second moment for the Hamiltonian

$$\mathcal{H} = \sum_i H_i^Z + \sum_{i<j} H_{ij},$$

where H_i^Z is the Zeeman Hamiltonian for spin $\vec{I}_i$ and H_{ij} has been defined in formula (8). He uses an electric quadrupole perturbation Hamiltonian similar to that given in formula (3) and obtains (see also Ref. 28)

$$\hbar^2 \langle \Delta \omega^2 \rangle_{\mathrm{NAR1}} = 2I(I+1) \sum_j A_{ij}^2 + 2I(I+1) \sum_j A_{ij} \bar{B}_{ij}$$
$$+ 3I(I+1) \sum_j \bar{B}_{ij}^2,$$

$$\hbar^2 \langle \Delta \omega^2 \rangle_{\mathrm{NAR2}} = 2I(I+1) \sum_j A_{ij}^2 - 4I(I+1) \sum_j A_{ij} \bar{B}_{ij}$$
$$+ 6I(I+1) \sum_j \bar{B}_{ij}^2,$$

$$\hbar^2 \langle \Delta \omega^2 \rangle_{\mathrm{NMR}} = 3I(I+1) \sum_j \bar{B}_{ij}^2. \qquad (10)$$

In formula (10) we have added the expression for the NMR second moment and $\bar{B}_{ij}$ is defined by

$$\bar{B}_{ij} = B_{ij} \frac{3 \cos^2 \bar{\theta}_{ij} - 1}{2}, \qquad (11)$$

where $\bar{\theta}_{ij}$ is the angle between $\vec{R}_{ij}$ and $\vec{H}_0$. It is thus possible, for each orientation of the magnetic field, to deduce $\sum_j A_{ij}^2$, $\sum_j A_{ij} \bar{B}_{ij}$, and $\sum_j \bar{B}_{ij}^2$ from the measured values of the second moments in solving the linear equations (10). As pointed out in the Introduction, we can then compare the measured and theoretical angular dependence of the parameters in spin Hamiltonian (8). Koloskova[15] has calculated the second moments for the Hamiltonian

$$\mathcal{H} = \sum_i H_i^Z + \sum_{i<j} H_{ij}^Q,$$

where H_{ij}^Q has been given in formula (9). In the case of an isotropic electric quadrupole spin Hamiltonian, we obtain

$$\hbar^2 \langle \Delta\omega^2 \rangle_{NAR1} = \hbar^2 \langle \Delta\omega^2 \rangle_{NAR2} = \tfrac{576}{5} I(I+1)[4I(I+1) - 3]$$

$$\times [4I(I+1) - 7] \sum_j C_{ij}^2, \qquad (12)$$

$$\hbar^2 \langle \Delta\omega^2 \rangle_{NMR} = \tfrac{96}{7} I(I+1)[4I(I+1) - 3]^2 \sum_j C_{ij}^2.$$

In a general second-moment expression, crossed terms involving the products $\sum_j A_{ij} C_{ij}$, $\sum_j \bar{D}_{ij} \bar{B}_{ij}$, etc. should also be included.

III. EXPERIMENTAL DETAILS AND RESULTS

A. Strain problems

The signals were observed with a conventional marginal oscillator ultrasonic spectrometer.[5] It records the derivative of the acoustic attenuation (caused by the absorption of energy by the nuclear spins) with respect to the magnetic field. Most of the pure niobium single crystals studied have been lent to us by the Oak Ridge National Lab. Some of them (orientation [100]) consist of cylinders about 6.7 mm in diameter and 9 mm in length. After cutting they were annealed at 2150 °C for 34 h at 2×10^{-9} Torr. Other crystals (orientation [110]) were supplied to us as cylinders about 6 mm in diameter and 25 mm in length. They had been annealed at 2300 °C for 50 h at 4×10^{-10} Torr. Their resistivity ratio and the density of dislocation lines was measured at Oak Ridge and found to be, respectively, 7500 and 10^4 lines per square centimeter. We then spark cut the crystals to convenient dimensions and lapped the faces to produce parallel faces. We give in Table II relevant information about some of the crystals that we measured. We also studied single crystals supplied by Westinghouse Corp. (resistivity ratio equal to 280) and by Bell Lab. (resistivity ratio equal to 1200); their linewidths were generally broader than those of the Oak Ridge single crystals.

It is well known by NMR measurements that niobium is very sensitive to strains or impurities in the metal. In powders,[29] NMR signals correspond only to the transition $-\tfrac{1}{2} \to \tfrac{1}{2}$ which is not broadened in first order by electric quadrupole interactions. This sensitivity of niobium to strains was the main experimental problem. We give in Fig. 1 the linewidths as a function of angle measured for samples Nos. 1, 2, 3, and 4. We have found that sample No. 1, which has neither been spark cut nor lapped, gave the same linewidths at 77 and 300 °K, while in samples Nos. 2, 3, 4, and 5 the linewidths broadened on decreasing the temperature. We estimate that it is due to strains which appear during the cooling process in crystals which had been slightly damaged during the cutting or polishing operations. The NAR1 line shapes are particularly strain dependent. We give in Fig. 2 NAR1 signals obtained at 300 and 77 °K with the same single crystal (No. 3). The structure at 77 °K can be partially explained if we assume that the single crystal has been given a longitudinal stress along the [001] axis. We show under the signals the positions and relative transition probabilities of the transitions m to $m - 1$ used to calculate the dashed curve, which is a superposition of Gaussian line shapes. Sundfors[28] has shown that for NAR1 the "outer" transitions have not only larger transition probabilities than the "inner" transitions, but that their linewidth is also smaller; we have used this result. Knowing the S-tensor components (see Sec. III B) it is possible to estimate the stress responsible for the splitting. We have found ~1 kg/mm^2 corresponding to a strain $\epsilon = 10^{-4}$. The NAR2 or NMR linewidths are less sensitive to the presence of strains, since in this case the "inner" probabilities are largest. We feel that the NAR technique as applied to the $\Delta m = \pm 1$ transition could thus be a useful tool in studying small strains in the volume of a single crystal.

Sample No. 1 was measured directly after annealing at 2150 °C for many hours. Given its high purity, it is thus expected that the measured linewidths and line shapes correspond to the intrinsic niobium signal, and in particular that it is not broadened by static electric quadrupole interactions. As can be seen on Fig. 1, samples Nos. 3 and 4 at 300 °K have the same linewidths as that of

TABLE II. Informations about the single crystals refered to in this paper.

Sample number	Cylinder axis	Supplier	Measured at	Spark cut	Lapped
1	[100]	Oak Ridge	Cal-Tech.	No	No
2	[100]	Oak Ridge	Cal-Tech.	No	Yes
3	[110]	Oak Ridge	Geneva	Yes	Yes
4	[110]	Oak Ridge	Geneva	Yes	Yes
5	[110]	Oak Ridge	Geneva	Yes	Yes
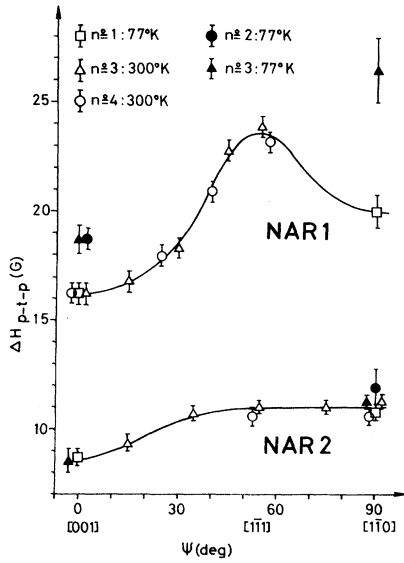
FIG. 1. Peak-to-peak linewidths for the electric quadrupole transitions $\Delta m = \pm 1$ (NAR1) and $\Delta m = \pm 2$ (NAR2). The magnetic field $\vec{H}_0$ rotates in the plane (110), ψ is the angle between [001] and $\vec{H}_0$. The sound-wave frequency $\nu \simeq 20$ MHz.

sample No. 1. Recently Leisure et al.[30] reported the observation of isotropic electric quadrupole broadening in single-crystal tantalum. We considered the possibility of such a broadening in niobium, which would add a fourth term to the second-moment expression given in formula (10). We shall show later (Sec. IV A) that the experimental data can be analyzed coherently only with the three
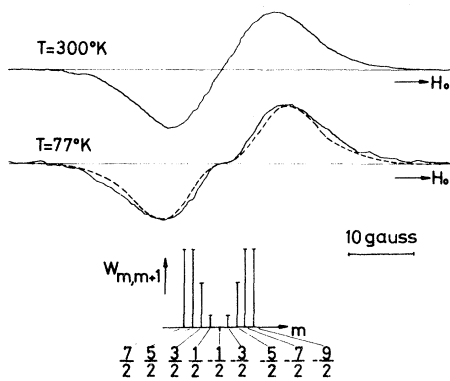
FIG. 2. Derivative of the nuclear-acoustic-attenuation coefficient of ^{93}Nb as a function of the magnetic field $\vec{H}_0$. The sound-wave vector $\vec{q}$ is along [110], the displacement vector $\vec{\xi}$ and $\vec{H}_0$ are along [001]. Sample No. 3, $\nu \simeq 20$ MHz, modulation field $= 2.8$ G peak to peak. Both signals correspond to an electric quadrupole transition $\Delta m = \pm 1$. The dashed curve is a superposition of Gaussian lineshapes, whose positions and relative intensities $W_{m,m+1}$ are given below the spectra.

terms given in formula (10). There is thus no experimental evidence suggesting that the quadrupole broadening is important and we shall assume that the linewidths for sample No. 1 and for samples Nos. 3 and 4 measured at 300 °K correspond to the unstrained linewidths and line shapes.

B. Gradient-elastic tensor

The S-tensor components S_{44} and $S_{11} - S_{12}$ are related to the nuclear-spin-dependent acoustic attenuation $\Delta \alpha_1$ and $\Delta \alpha_2$ through Eq. (6). $\Delta \alpha_1$ and $\Delta \alpha_2$ are proportional to the line-shape factor $g(\nu)$ which is angular dependent. This line-shape angular dependence drops out when $\Delta \alpha$ is integrated over ν, we are thus interested in the experimental quantity $\int \Delta \alpha \, dH$ whose value is more easily related to the efg-strain tensor. Sundfors[7] has described the method used to measure the absolute value of $\Delta \alpha$. The idea is to simulate with a known calibration signal ΔG_{cal} the conductance change ΔG_{signal} at the grid of the oscillator tube of the marginal oscillator. We then have

$$\int \Delta \alpha \, dH = \frac{C \alpha R_a}{H_m} \int_0^\infty dH \int_0^H \frac{\Delta G_{signal}}{\Delta G_{cal}} dH,$$

where C is a constant depending on the characteristic of the calibrator, α is the background attenuation coefficient, H_m is the amplitude of the low-frequency modulation field used to display the derivative of $\Delta \alpha$. R_a is the equivalent series resistance of the composite resonator formed by the crystal and the transducer bonded to it. In order to improve the sensitivity and to integrate the derivative of $\Delta \alpha$ we used a signal averager. The accuracy of the calibrator was checked in measuring $\int \Delta \alpha \, dH$ for the NAR signal due to magnetic dipole coupling, whose magnitude can be exactly calculated.

The measurements were done with samples Nos. 3 and 5 which are both orientated along [110]. To avoid the superposition of the magnetic dipole NAR signal and the electric quadrupole NAR signal we used a geometry in which $\vec{H}_0$ rotates in a plane perpendicular to the sound-wave vector. In this case, for a displacement vector along [001], the angular dependences $f_1^2(\psi)$ and $f_2^2(\psi)$ of $\Delta \alpha_1$ and $\Delta \alpha_2$ are, respectively, equal to $4(S_{44})^2 \cos^2\psi$ and $4(S_{44})^2 \sin^2\psi$ (see Table I). We report in Fig. 3 the values of $\int \Delta \alpha \, dH$ as a function of the angle ψ. The agreement with the theoretical angular factor is good and shows that the interaction mechanism is indeed the electric quadrupole mechanism.

The experimental values of S_{44} and $S_{11} - S_{12}$ as well as theoretical values calculated on the basis of a point charge model are given in Table III. The quoted S_{44} is the mean value of measurements done
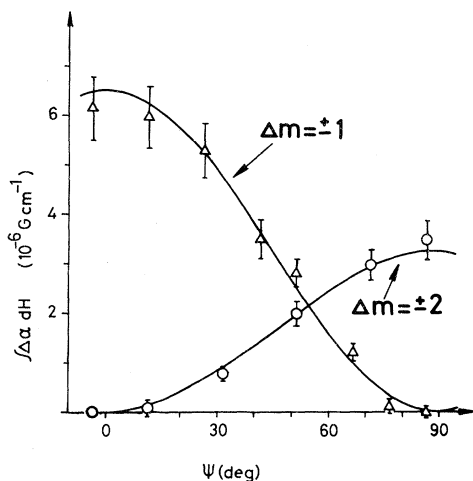
FIG. 3. $\int \Delta\alpha\, dH$ as a function of the angle ψ between $\vec{H}_0$ and $\lfloor 001 \rfloor$ for the transitions $\Delta m = \pm 1$ and $\Delta m = \pm 2$. Sample No. 3, $\vec{q} // [110]$, $\vec{\xi} // [001]$, $\vec{H}_0$ in plane (110), $\nu \simeq 20$ MHz, $T = 300$ °K. The full curves are the $\cos^2\psi$ and $\sin^2\psi$ theoretical angular dependences in this geometry.

at 300 and 77 °K for the $\Delta m = \pm 1$ and $\Delta m \pm 2$ transitions; the quoted $S_{11} - S_{12}$ was only measured at 77 °K for sensitivity reasons. The point charge values were calculated using a planewise summation method[8] with the relations

$$(S_{11} - S_{12})_{\text{latt}} = \tfrac{3}{2} S_{11\,\text{latt}}$$

and

$$S_{44\,\text{latt}} = -\tfrac{1}{2} S_{11\,\text{latt}}$$

where

$$S_{11\,\text{latt}} = (Z \mid e \mid a^{-3}) 5.758 .$$

a is the lattice spacing and Z is the positive charge of a neighboring ion. (In Ref. 8, S_{11} should be opposite in sign in all formulas.) By analogy with the static efg,[31] we split the S-tensor components into two parts (e.g., for S_{12} and S_{44})

$$S_{11} = S_{11\,\text{latt}} (1 - \gamma_\infty) + S_{11\,\text{ce}} (1 - R),$$

where $S_{11\,\text{ce}}$ is the contribution of conduction elec-

trons inside an atomic sphere centered at the nuclear site, γ_∞ is the familiar Sternheimer antishielding factor, and R is the shielding factor. The large ratio between the measured and point charge S-tensor components reflects the dominant contribution of the conduction electrons.

C. Second moments

For a given orientation of $\vec{H}_0$ the NAR$_{\text{dip}}$, NAR1, and NAR2 experimental lines may be different. We show in Fig. 4 three such resonance signals for an orientation $[1\bar{1}1]$ of the magnetic field. The NAR dipolar line is in fact the superposition of a pure magnetic-dipole-coupled signal which has the same line as a standard NMR signal and a negligibly small electric-quadrupole-coupled signal. In order to verify this result Descouts[32] measured one of our niobium single crystals at 300 °K with a standard Varian NMR crossed-coil spectrometer. He adjusted the paddles to get a symmetric signal and obtained line shapes similar to that measured by nuclear acoustic resonance.[33] The determination of second moments is difficult since the tails of the signal give a large contribution. We integrated by a Simpson-rule method the derivative of the acoustic attenuation coefficient and, after adjustment of the base line to get a symmetric first integral, we again used a Simpson-rule method to calculate the second moment. For the NAR1 and NAR2 signals we also fitted the line shapes with an analytical expression

$$g(H) = A e^{-[(H - H_0)/\Delta H]^p} ,$$

where the exponent p is near 2. For the NAR dipolar line shape the fitting is not as good and the error bars are larger. The second-moment results are summarized in Table IV, we also give the exponent p used in fitting the line shapes.

IV. ANALYSIS OF THE SECOND MOMENTS

From the experimental second moments given in Table IV, $\sum_j A_{ij}^2$, $\sum_j A_{ij}\bar{B}_{ij}$, and $\sum_j \bar{B}_{ij}^2$ are obtained in solving the system of linear equations (10). The results are summarized in Fig. 5 for the

TABLE III. Experimental and point-charge theoretical results ($Z = +1$, $a = 3.3004$ Å) for the S-tensor components in niobium. The S-tensor coefficients are given in units of statcoulomb cm^{-3} and the products $\mid QS \mid$ in units of statcoulomb cm^{-1}. The value of the electric quadrupole moment $Q = 0.2$ b.

$\mid QS_{44} \mid_{\text{meas}} = 4.5 \times 10^{-9}$ ($\pm 15\%$)	$\mid Q\,(S_{11} - S_{12}) \mid_{\text{meas}} = 2.4 \times 10^{-9}$ ($\pm 15\%$)
$\mid S_{44} \mid_{\text{meas}} = 2.25 \times 10^{16}$	$\mid S_{11} - S_{12} \mid_{\text{meas}} = 1.2 \times 10^{16}$
$S_{44\,\text{latt}} = -3.85 \times 10^{13}$	$(S_{11} - S_{12})_{\text{latt}} = 1.15 \times 10^{14}$
$\dfrac{S_{44\,\text{meas}}}{S_{44\,\text{latt}}} = \pm 584$	$\dfrac{(S_{11} - S_{12})_{\text{meas}}}{(S_{11} - S_{12})_{\text{latt}}} = \pm 104$
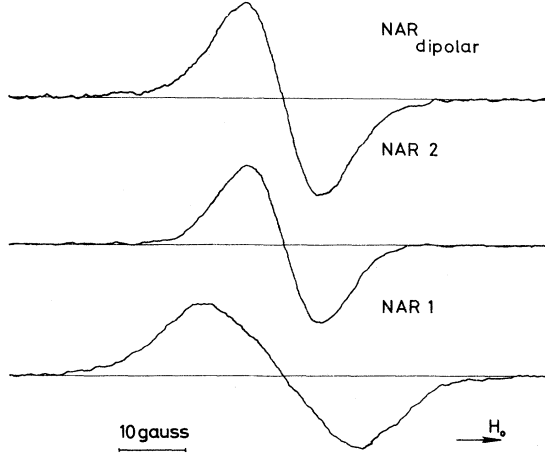
FIG. 4. Derivative of the nuclear-acoustic-attenuation coefficient of ^{93}Nb. Sample No. 3, $\vec{q} \,/\!/\,[110]$, $\vec{H}_0 \,/\!/\,[1\bar{1}1]$, $\nu \simeq 20$ MHz; $\vec{\xi} \,/\!/\,[1\bar{1}0]$ and $T = 15\,°$K for NAR$_{dip}$, $\vec{\xi} \,/\!/\,[001]$ and $T = 300\,°$K for NAR1 and NAR2, modulation field $= 2.8$ G peak to peak.

orientations $[001]$, $[1\bar{1}1]$, and $[1\bar{1}0]$ of the magnetic field. We have assumed in calculating these values that the Hamiltonian (8) contains all the broadening mechanisms in niobium. This assumption can be verified by comparing the predicted angular dependences of $\sum_j A_{ij}^2$, $\sum_j A_{ij}\overline{B}_{ij}$, and $\sum_j \overline{B}_{ij}^2$ with the measured values. $\sum_j A_{ij}^2$ should be constant for all orientations of $\vec{H}_0$ since A_{ij} is a function of R_{ij} only. $\sum_j A_{ij}\overline{B}_{ij}$ can be written by using the addition theorem for spherical harmonics Y_{1m}:

$$\sum_j A_{ij}\overline{B}_{ij} = \frac{4\pi}{5}\sum_{m=-2}^{+2} Y_{2m}(\theta, \phi)$$

$$\sum_j A_{ij}B_{ij}Y_{2m}^{*}(\theta_{ij}, \phi_{ij}),$$

where θ, ϕ and θ_{ij}, ϕ_{ij} are, respectively, the polar angles of $\vec{H}_0$ and $\vec{R}_{ij}$ in the system of axis $[100]$, $[010]$, and $[001]$. The sum over j vanishes when taken on a shell p around the nucleus i and thus $\sum_j A_{ij}\overline{B}_{ij} = 0$. O'Reilly and Tsang[34] have calculated the most general angular variation of $\sum_j \overline{B}_{ij}^2$ in a cubic structure. They obtain

$$\sum_j \overline{B}_{ij}^2 = P(x^4 + y^4 + z^4 - Q), \tag{13}$$

where P and Q are two independent parameters and x, y, z are the direction cosines specifying the orientation of the magnetic field with respect to the crystallographic axes. In the case where $\vec{H}_0$ rotates in the (110) plane, we have

$$\sum_j \overline{B}_{ij}^2 = P(\tfrac{3}{2}\cos^4\psi - \cos^2\psi + \tfrac{1}{2} - Q). \tag{14}$$

We give in Fig. 5 the best fit for $\sum_j A_{ij}^2$, $\sum_j A_{ij}\overline{B}_{ij}$, and $\sum_j \overline{B}_{ij}^2$ in keeping with the predicted angular dependences. It corresponds to

$$\sum_j (A_{ij}/\hbar)^2 = 1.14 \pm 0.25 \text{ kHz}^2,$$

$$\sum_j (\overline{B}_{ij}/\hbar)^2 = -0.840(x^4 + y^4 + z^4 - 1.20) \text{ kHz}^2,$$

$$\sum_j (A_{ij}/\hbar)(\overline{B}_{ij}/\hbar) = 0.03 \pm 0.13 \text{ kHz}^2.$$

TABLE IV. Second moments of ^{93}Nb in niobium single crystals for NAR$_{dip}$(NMR), NAR1, and NAR2 resonance signals. The pure theoretical dipole-dipole contribution is also given as well as second-moment data taken from Schone's work (Ref. 19).

	[001]	[1$\bar{1}$1]	[1$\bar{1}$0]
NMR (Ref. 19)			
ΔH_{p-t-p} (G)	4.3	$\cdots$	9.1
$\langle \Delta H^2 \rangle$ (G^2)	11.1 ± 3	$\circ \cdot \cdot$	46.3 ± 7.5
dipolar (G^2)	10.2	19.7	17.3
NAR$_{dip}$			
Sample (T °K)	4 and 5 (~ 15 °K)	4 and 5 (~ 15 °K)	3 and 5 (~ 15 °K)
ΔH_{p-t-p} (G)	3.9 ± 0.3	11.0 ± 0.5	8.6 ± 0.5
Exponent p	~ 1.6	~ 1.75	~ 1.70
$\langle \Delta H^2 \rangle$ (G^2)	12 ± 3	50 ± 8	40 ± 8
NAR1			
Sample (T °K)	1(77 °K) and 4(300 °K)	4(300 °K)	1(77 °K)
ΔH_{p-t-p} (G)	16.2 ± 0.5	23.0 ± 0.6	20 ± 0.8
Exponent p	$1.9 - 1.95$	$2.3 - 2.4$	2.15
$\langle \Delta H^2 \rangle$ (G^2)	75 ± 7	96 ± 8	92 ± 6
NAR2			
Sample (T °K)	1(77 °K)	4(300 °K)	1(77 °K) and 3(300 °K)
ΔH_{p-t-p} (G)	8.9 ± 0.5	10.6 ± 0.4	10.9 ± 0.4
Exponent p	1.95	1.95	1.95
$\langle \Delta H^2 \rangle$ (G^2)	20 ± 2.5	34 ± 4	34 ± 4
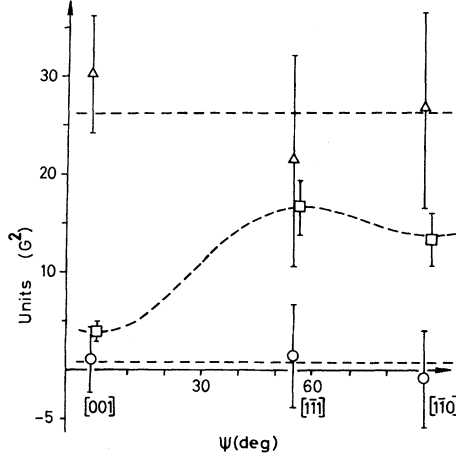
FIG. 5. Angular dependence of $I(I+1)(\gamma\hbar)^{-2}\sum_j A_{ij}^2$ (triangles), $I(I+1)(\gamma\hbar)^{-2}\sum_j A_{ij}\bar{B}_{ij}$ (circles), and $I(I+1)(\gamma\hbar)^{-2}\sum_j \bar{B}_{ij}^2$ (squares). The error bars represent the maximum errors given by the values in Table IV. The dashed lines are the best fit in keeping with the predicted angular dependences (see text).

The agreement is excellent for $\sum_j A_{ij}\bar{B}_{ij}$ and $\sum_j \bar{B}_{ij}^2$ and within error margin for $\sum_j A_{ij}^2$. We thus conclude from our data that there is no clear experimental evidence suggesting that the Hamiltonian (8) has to be completed by other terms. The effect of the electric quadrupole term in particular seems to be small. In what follows we will analyze in more detail the exchange and pseudodipolar terms and give an order of magnitude of the electric quadrupolar contribution to the second moment.

A. Exchange and pseudodipolar terms

The dipolar Hamiltonian is the sum of a classical dipole-dipole interaction and a pseudodipolar interaction, we thus write

$$B_{ij} = \frac{\gamma^2\hbar^2}{R_{ij}^3} + B_{ij}^{PD} = \frac{\gamma^2\hbar^2}{R_{ij}^3}(1+b_{ij}), \qquad (15)$$

where b_{ij} is the same for all atoms belonging to a

TABLE V. Result of computer calculation of $\sum_{j\subset p} (a/R_{ij})^6 S_{ij}$ for the first five shells and sum of these contributions for the first 25 shells.

shell	$\sum\limits_{j\subset p} (a/R_{ij})^6 S_{ij}$
1	$-9.48\ (\sigma-1)$
2	$4.5\ (\sigma-0.33)$
3	$-0.23\ (\sigma-1.67)$
4	$0.19\ (\sigma+0.64)$
5	$-0.15\ (\sigma-1)$
$1\to25$	$-5.19\ (\sigma-1.71)$

given shell p. Following the analysis made by Schratter and Williams[35] in the case of lead, we have

$$\sum_j \bar{B}_{ij}^2 = \sum_j B_{ij}^2 \left(\frac{3\cos^2\bar{\theta}_{ij}-1}{2}\right)^2 = \sum_j B_{ij}^2 S_{ij},$$

$$S_{ij} = 1.875(o_{ij}-0.6)\sigma - 1.125\sigma_{ij}+0.875,$$

where $\sigma_{ij} = (X_{ij})^4+(Y_{ij})^4+(Z_{ij})^4$ refers to the direction cosines made by $\vec{R}_{ij}$ and σ to those made by $\vec{H}_0$ with the crystallographic axes. In summing the j atoms belonging to a given shell p

$$\sum_j \bar{B}_{ij}^2 = \frac{\gamma^4\hbar^4}{a^6}\sum_p (1+b_p)^2 \sum_{j\subset p}\left(\frac{a}{R_{ij}}\right)^6 S_{ij}, \qquad (16)$$

where $b_p = b_{ij}$ if the j atom belongs to the p shell around the nucleus i.

We have calculated the expression $\sum_{j\subset p}(a/R_{ij})^6 \times S_{ij}$ in the case of a bcc crystal structure. We show in Table V the result for the first five shells. The angular dependence of $\sum_{j\subset p}(a/R_{ij})^6 S_{ij}$ for $p=1$ and $p=2$ are given in Fig. 6. We have also drawn the contribution to $\sum_j \bar{B}_{ij}^2$ of the classical dipole-dipole term, and the measured $\sum_j \bar{B}_{ij}^2$. It is important to note that when $\vec{H}_0$ is along [001] the shell No. 1 does not contribute to the second moment and the shell No. 2 contributes 80% of the classical dipole-dipole term (approximately equal to the contribution of the first 25 shells). The situation is opposite when $\vec{H}_0$ is oriented along [1$\bar{1}$1] where shell No. 2 does not contribute to the second moment. If we make the simplifying assumption that $b_3 = b_4 = \cdots = b$, we can calculate $|1+b_1|$ and $|1+b_2|$ under different conditions. $|1+b_1|$ will be mainly determined by the value of $\sum_j \bar{B}_{ij}^2$ when $\vec{H}_0$ is along [1$\bar{1}$1] and $|1+b_2|$ when $\vec{H}_0$ is along [001]. The results are summarized in Table VI, $|1+b_1|$ and $|1+b_2|$ do not strongly depend on the assumptions made. We estimate therefore

$$|1+b_1| = 1.6\pm0.2,$$

$$|1+b_2| = 1.0\pm0.2,$$

corresponding to the pseudodipolar coupling constants B_{ij}^{PD}:

$$B_1^{PD}/h = 184\pm60 \text{ Hz or } -800\pm60 \text{ Hz},$$

$$B_2^{PD}/h = 0\pm40 \text{ Hz or } -400\pm40 \text{ Hz}.$$

To our knowledge no detailed calculation of the pseudodipolar interaction in niobium has been published. There is no a priori reason to choose one particular set of values for B_1^{PD} and B_2^{PD}.

Rudermann and Kittel[9] gave an analytical expression for the exchange constant $A_{ij}(R_{ij})$ in the case of a free-electron model and showed that at large distance A_{ij} decreases like $R_{ij}^{-3}\cos(2k_F R_{ij})$ where k_F is the Fermi wave vector. As R_{ij} increases the

contribution to $\sum_j A_{ij}^2$ from the corresponding shells diminishes therefore rapidly. Nevertheless it is difficult to assign a given value even to the first shell since the oscillatory behavior may cancel out A_{ij}. If we assume that only A_1 is nonzero we obtain $A_1/\hbar = 378$ Hz; if A_{ij} is assumed to be proportional to R_{ij}^{-3} we obtain $A_1/\hbar \simeq 300$ Hz.

B. Electric quadrupolar term

An estimation of the contribution to the second moment by the effective electric quadrupole Hamiltonian H_{ij}^Q [see Eq. (9)] is difficult since it depends on the details of the wave functions at the Fermi surface. In what follows we will first estimate the electric quadrupole relaxation rate in ^{93}Nb by comparison with its known value in ^{97}Mo.[27] The ratio between the electric quadrupole and exchange contributions to the second moment is then calculated using a formula derived from Kessel's work,[14] which relates the relaxation rates to the effective spin Hamiltonians.

Narath and Aldermann[27] showed that the different relaxation rates for ^{95}Mo and ^{97}Mo could be explained by the different electric quadrupole moments of the two isotopes. They were thus able to measure the relaxation rate constant $R^Q = 1/T_1^Q T$, where T_1^Q is the electric quadrupole relaxation time calculated by Mitchell[24] in the free-electron model and by Obata[36] in the tight-binding approximation. Using Obata's expressions for R^Q and R^μ, where R^μ is the usual Fermi contact relaxation rate, we obtain

FIG. 6. Angular dependence of $\sum_{j \subset p} (a/R_{ij})^6 S_{ij}$ as defined in the text. The dashed curve is the best fit to the measured $\sum_j \bar{B}_{ij}^2$ (in units of $\gamma^4 \hbar^4/a^6$) in keeping with the predicted angular dependence.

$$\frac{(R^Q/R^\mu)_{\text{Mo}}}{(R^Q/R^\mu)_{\text{Nb}}} \simeq 4.3 \left(\frac{Q_{\text{Mo}}}{Q_{\text{Nb}}} \right)^2 \left(\frac{\gamma_{\text{Nb}}}{\gamma_{\text{Mo}}} \right)^2 \left(\frac{N_{d\,\text{Mo}}}{N_{d\,\text{Nb}}} \right)^2 \left(\frac{N_{s\,\text{Nb}}}{N_{s\,\text{Mo}}} \right)^2$$

$$\times \left(\frac{H_{\text{hfs Nb}}}{H_{\text{hfs Mo}}} \right)^2 \left(\frac{\langle r^{-3} \rangle_{\text{Mo}}}{\langle r^{-3} \rangle_{\text{Nb}}} \right)^2 , \qquad (17)$$

where N_s, N_d are the densities of state at the Fermi surface for band s and d, respectively, H_{hfs} is the contact hyperfine field in the metal. With the values for molybdenum and niobium given, respectively, in Refs. 27 and 37, we calculate $(R^Q/R^\mu)_{\text{Mo}}/(R^Q/R^\mu)_{\text{Nb}} = 1360$ giving $(R^Q/R^\mu)_{\text{Nb}} = 1.7 \times 10^{-4}$. Kessel pointed out that in the free-electron approximation the coefficients A_{ij} and C_{ij} in the bilinear (8) and electric quadrupole (9) spin Hamiltonian are related through the relaxation rates

$$\frac{C_{ij}}{A_{ij}} = \frac{12}{(2I+3)(2I-1)} \left(\frac{R^Q}{R^\mu} \right) \frac{\beta_2(z_{ij})}{\alpha(z_{ij})} , \qquad (18)$$

where $z_{ij} = 2k_F R_{ij}$, $\alpha(z_{ij})$ and $\beta_2(z_{ij})$ are oscillatory functions of z_{ij} (given by Kessel) whose ratio is typically between 1 and 10. Using formulas (10), (12), and (18) we then have for a spin $\frac{9}{2}$ and the transition NAR1

$$\frac{\hbar^2 \langle \Delta\omega^2 \rangle_{\text{quadr}}}{\hbar^2 \langle \Delta\omega^2 \rangle_{\text{exch}}} \simeq 7950 \left(\frac{R^Q}{R^\mu} \right)^2 \frac{\sum_j [\beta_2(z_{ij})]^2}{\sum_j [\alpha(z_{ij})]^2} . \qquad (19)$$

Substituting the value for R^Q/R^μ deduced above we obtain, with $\beta_2(z_{ij})/\alpha(z_{ij}) = 0.1$,

$$\frac{\hbar^2 \langle \Delta\omega^2 \rangle_{\text{quadr}}}{\hbar^2 \langle \Delta\omega^2 \rangle_{\text{exch}}} = 2.3 \times 10^{-6} .$$

This contribution is too small to alter measurably the second moment. It should, however, be noted that formula (19) gives only an order-of-magnitude estimate of the ratio of quadrupole and exchange contributions to the second moment. In particular it is derived from Eq. (17) which is valid only in the tight-binding approximation and for a shielding factor R equal to zero, and from Eq. (18) which is valid only in the free-electron approximation and for p-type wave functions at the Fermi surface. It was also shown in Sec. III B that the conduction-electron part $S_{11\,\text{ce}}$ of the efg-strain tensor is very large in niobium. An enhancement of the niobium efg relative to that of molybdenum by a factor of 8–25 would give a quadrupole contribution to the

TABLE VI. Experimental values of $|1+b_1|$ and $|1+b_2|$ under different assumptions on $b_3 = b_4 = \cdots = b$.

Assumption on b	$|1 = b_1|$	$|1+b_2|$
None	1.51 ± 0.34	$\cdots$
$|1+b| = 0$	1.71 ± 0.14	1.21 ± 0.13
$|1+b| = |1+b_1|$	1.60 ± 0.11	0.92 ± 0.24
$|1+b| = |1+b_2|$	1.66 ± 0.16	1.09 ± 0.24

second moment equal to the exchange one.

In the case of ^{97}Mo where $R^Q/R^\mu = 0.23$, a formula similar to (19) gives for the NMR line shape, if we take only into account the interactions between ^{97}Mo nuclei:

$$\frac{\hbar^2 \langle \Delta\omega^2 \rangle_{\text{quadr}}}{I(I+1)\sum_j A_{ij}^2} = 104 \frac{\sum_j [\beta_2(z_{ij})]^2}{\sum_j [\alpha(z_{ij})]^2}.$$

Narath and Aldermann found that the spin echo signal in ^{97}Mo is narrower than in ^{95}Mo, which has a smaller electric quadrupole moment. They interpreted this as the effect of static strains in the powder. An alternative explanation is to suggest that the echo signal is narrower in ^{97}Mo due to the effective electric quadrupole Hamiltonian H_{ij}^Q.

V. CONCLUSION

Our study of nuclear acoustic resonance in single-crystal niobium has shown that the NAR technique gives more information on the indirect spin Hamiltonian between nuclear spins than the conventional NMR technique. This is borne out by the following two remarks: First, the NAR line shapes are different for the $\Delta m = 1$ and $\Delta m = 2$ electric quadrupole transition and for the $\Delta m = 1$ magnetic dipole transition; second, the second moments depend not only on the dipolar term, as in NMR, but also on the exchange term. In the case of niobium this allowed us to verify that a spin Hamiltonian equal to the sum of an exchange and dipolar term is consistent with the measurements. We also obtained values for the first- and second-nearest-neighbor-shell pseudodipolar coefficients and for

the pseudoexchange coefficient. Using a formula derived from Kessel's work the contribution to the second moment of the indirect electric quadrupole spin Hamiltonian has been evaluated. Its effect has been found to be weak in niobium, it is not however negligible in molybdenum. From measurements of the absolute intensity of the NAR signal it is possible to measure the coefficients of the efg-strain tensor. We found the values of $|S_{11} - S_{12}|$ and $|S_{44}|$ in niobium and showed that they are much larger than the point charge values.

To our knowledge no detailed calculation of the S-tensor components has been attempted in a metal and only in the case of lead[38] were the indirect interaction coefficients calculated in a d-band metal. Both the pseudoexchange, pseudodipolar, and efg-strain tensor depend on the details of the wave functions and comparison between measured and calculated values could serve as a good test of the present band-structure calculations in niobium.[39]

*Present address: Ecole Polytechnique Fédérale de Lausanne, Laboratoire de physique expérimentale, 1000 Lausanne, Switzerland.

[1] E. F. Taylor and N. Bloembergen, Phys. Rev. 113, 431 (1959).

[2] H. J. Hackeloer and O. Kanert, Z. Naturforsch. A 27, 1235 (1972).

[3] O. Kanert and K. Preusser, Phys. Status Solidi A 15, 483 (1973).

[4] J. R. Anderson and J. S. Karra, Phys. Rev. B 5, 4334 (1972).

[5] D. I. Bolef and M. Menes, Phys. Rev. 114, 1441 (1959).

[6] D. I. Bolef, in Physical Acoustics, edited by W. P. Mason (Academic, New York, 1969), Vol. IV A.

[7] R. K. Sundfors, Phys. Rev. 177, 1221 (1969).

[8] J. Buttet, J. Phys. F 3, 918 (1973).

[9] M. A. Ruderman and C. Kittel, Phys. Rev. 96, 99 (1954).

[10] N. Bloembergen and T. J. Rowland, Phys. Rev. 97, 1679 (1955).

[11] J. H. Van Vleck, Phys. Rev. 74, 1168 (1948).

[12] H. Alloul and C. Froidevaux, Phys. Rev. 163, 324 (1967).

[13] R. Loudon, Phys. Rev. 119, 919 (1960).

[14] A. R. Kessel, Fiz. Met. Metalloved. 23, 837 (1967).

[15] N. G. Koloskova, Fiz. Met. Metalloved. 15, 137 (1963).

[16] D. H. McMahon and R. H. Silsbee, Phys. Rev. 135, A91 (1964).

[17] J. Buttet and E. H. Gregory, Phys. Lett. A 33, 265 (1970).

[18] J. Buttet, Solid State Commun. 9, 1129 (1971).

[19] H. E. Schone, Phys. Rev. 183, 410 (1969).

[20] R. V. Pound, Phys. Rev. 79, 685 (1950).

[21] R. J. Harrison and P. L. Sagalyn, Phys. Rev. 128, 1630 (1962).

[22] W. D. Smith, thesis (Washington University, St. Louis, 1970) (unpublished).

[23] J. Buttet, E. H. Gregory, and P. K. Baily, Phys. Rev. Lett. 23, 1030 (1969).

[24] A. H. Mitchell, J. Chem. Phys. 26, 1714 (1957).

[25] S. D. Mahanti and T. P. Das, Phys. Rev. 170, 426 (1968).

[26]L. L. Hirst (private communication).

[27]A. Narath and D. W. Alderman, Phys. Rev. 143, 328 (1966).

[28]R. K. Sundfors, Phys. Rev. 185, 458 (1969).

[29]J. Butterworth, Proc. Phys. Soc. Lond. 85, 735 (1965).

[30]R. G. Leisure, D. K. Hsu, and B. A. Seiber, Phys. Lett. A 42, 195 (1972).

[31]R. E. Watson, A. C. Gossard, and Y. Yafet, Phys. Rev. 140, A375 (1965).

[32]P. Descouts (private communication).

[33]The magnetic-dipole-coupled NAR line shapes are symmetric at low temperature. This is not the case for the NMR line shapes which are a mixture of absorption and dispersion in a single crystal. A symmetric line shape is obtained if we purposely add a dispersive component canceling the dispersive part of the NMR signal.

[34]D. E. O'Reilly and T. Tsang, Phys. Rev. 128, 2639 (1962).

[35]J. Schratter and D. L. Williams, Phys. Rev. B 5, 4302 (1972).

[36]Y. Obata, J. Phys. Soc. Jpn. 19, 2348 (1964).

[37]Y. Yafet and V. Jaccarino, Phys. Rev. 133, A1630 (1964).

[38]L. Tterlikkis, S. D. Mahanti, and T. P. Das, Phys. Rev. Lett. 21, 1796 (1968).

[39]J. R. Anderson, D. A. Papaconstantopoulos, J. W. McCaffrey, and J. E. Schirber, Phys. Rev. B 7, 5115 (1973).